DALTON
FULL PAPER

# Hydrothermal syntheses, structures and properties of terephthalate-bridged polymeric complexes with zig-zag chain and channel structures

**Daofeng Sun, Rong Cao,* Yucang Liang, Qian Shi, Weiping Su and Maochun Hong***

*State Key Laboratory of Structural Chemistry, Fujian Institute of the Research on the Structure of Matter, Chinese Academy of Sciences, Fujian, Fuzhou 350002, China*

***Received 29th March 2001, Accepted 11th June 2001***

Hydrothermal reactions of 1,4-dicyanobenzene, phen and M(OAc)$_2$ (M = Co, Zn) or MCl$_2$ (M = Cu, Mn, Cd) gave rise to the hydrolysis of 1,4-dicyanobenzene into terephthalic acid and the formation of five polymeric complexes [M(ta)(phen)(H$_2$O)]$_n$ (M = Co, **1**; Zn, **3**), [Cu(ta)(phen)]$_n$ (**2**), [Mn(ta)(phen)]$_n$ (**4**), [Cd(ta)$_{1/2}$(phen)Cl]$_n$ (**5**) (ta = terephthalate, phen = 1,10-phenanthroline). Crystal structure analyses revealed that complexes **1**–**3** have 1D zig-zag chain structures, and **4** and **5** possess 3D network structures with channels. Magnetic susceptibility measurements for **1**, **2** and **4** were consistent with the occurrence of weak antiferromagnetic interaction through the ta bridge.

## Introduction

With the aim of understanding the correlation between structure and magnetism, much attention has been paid to the architecture of polymeric magnetic systems, especially two- and three-dimensional systems.[1] The key step of the architecture of polymeric transition metal complexes is to select suitable multidentate bridging ligands.[2] Accordingly, multi-carboxylic ligands with suitable spacers are good choices for such architectures, especially benzoic acid-based ligands;[3–5] for instance, terephthalates (ta) have been used in many synthetic systems because they can form short bridges *via* one carboxylato end or long bridges *via* the benzene ring, leading a great variety of structures.[6,7] Scheme 1 summarizes some typical coordination modes for ta.[2]

Although a series of polymeric complexes containing the ta ligand has been reported, uncharacterised polymers were often obtained in conventional solution reactions. Considering the advantage of hydrothermal synthesis,[8–10] we recently began work on the construction of polymeric complexes by hydrothermal reactions of ta, phen and metal salts; unfortunately, only uncharacterised precipitates or microcrystals were isolated. Because the cyano group on the phenyl ring is easily transformed to a carboxylic group *via* hydrolysis reaction,[6,11] we replaced terephthalate by 1,4-dicyanobenzene and isolated a dinuclear complex [Cu$_2$(phen)$_4$(ta)][ClO$_4$]$_2$ from the reaction involving Cu(ClO$_4$)$_2$.[12] After introducing metal halides and acetates into the reactions, five polymeric complexes [Co(ta)(phen)(H$_2$O)]$_n$ **1**, [Cu(ta)(phen)]$_n$ **2**, [Zn(ta)(phen)(H$_2$O)]$_n$ **3**, [Mn(ta)(phen)]$_n$ **4**, and [Cd(ta)$_{1/2}$(phen)Cl]$_n$ **5** were successfully isolated. Reported herein are the details of their syntheses and characterizations.

## Experimental

### Preparation of complexes

**[Co(ta)(phen)(H$_2$O)]$_n$ 1.** A mixture of Co(CH$_3$CO$_2$)$_2$·4H$_2$O (0.25 g, 1 mmol), 1,4-dicyanobenzene (0.13 g, 1 mmol), 1,10-phenanthroline (0.4 g, 2 mmol) and H$_2$O (16 ml) in the molar ratio of *ca.* 1 : 1 : 2 : 889 was sealed in a 25 ml stainless-steel reactor with Teflon liner and was heated at 170 °C for 72 h. After cooling, rhombic, violet–red crystals of **1** were collected by filtration. Yield: 70%. Anal. Calc. for C$_{20}$H$_{14}$CoN$_2$O$_5$: C, 57.02; H, 3.32; N, 6.65%. Found: C, 57.03; H, 3.41; N, 6.76%. IR (KBr, cm$^{-1}$): 3385(br, vs), 1572(vs), 1369(vs), 1147(m), 839(s), 812(s), 723(s).

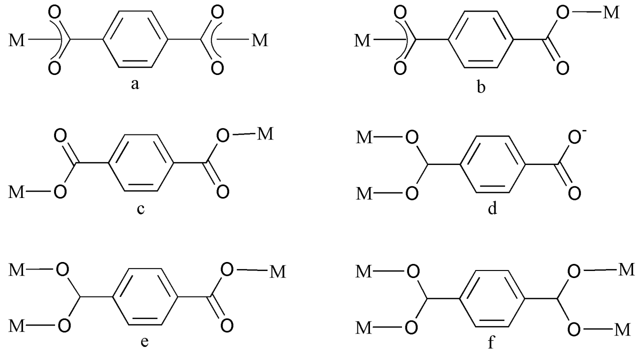

**Scheme 1** Typical coordination modes for the ta ligand.

**[Cu(ta)(phen)]$_n$ 2.** A mixture of CuCl$_2$·2H$_2$O (0.08 g, 0.5 mmol), 1,4-dicyanobenzene (0.065 g, 0.5 mmol), 1,10-phenanthroline (0.1 g, 0.5 mmol) and H$_2$O (16 ml) in the molar ratio *ca.* 1 : 1 : 1 : 1777 was sealed in a 25 ml stainless-steel reactor with Teflon liner and was heated at 130 °C for 72 h. After cooling, block-shaped, black–blue crystals of **2** were collected by filtration. Yield: 65%. Anal. Calc. for C$_{20}$H$_{12}$CuN$_2$O$_4$: C, 58.89; H, 2.94; N, 6.87%. Found: C, 58.72; H, 2.94; N, 6.98%. IR (KBr, cm$^{-1}$): 3385(br, vs), 1614(vs), 1605(vs), 1516(s), 1421(s), 1371(s), 1344(vs), 850(m), 825(s), 742(s), 723(m).

**[Zn(ta)(phen)(H$_2$O)]$_n$ 3.** A mixture of Zn(CH$_3$CO$_2$)$_2$·2H$_2$O (0.11 g, 0.5 mmol), 1,4-dicyanobenzene (0.065 g, 0.5 mmol), 1,10-phenanthroline (0.1 g, 0.5 mmol) and H$_2$O (16 ml) in the molar ratio of *ca.* 1 : 1 : 1 : 1777 was sealed in a 25 ml stainless-steel reactor with Teflon liner and was heated at 170 °C for 72 h. After cooling, block, colorless crystals of **3** were collected by filtration. Yield: 59%. Anal. Calc. for C$_{20}$H$_{14}$ZnN$_2$O$_5$: C, 56.17; H, 3.27; N, 6.54%. Found: C, 56.22; H, 3.30; N, 6.63%. IR (KBr, cm$^{-1}$): 3385(br, vs), 1612(vs), 1391(s), 1358(s), 1284 (m), 1038(m), 768(s), 517(m).

**[Mn(ta)(phen)]$_n$ 4.** A mixture of MnCl$_2$·4H$_2$O (0.1 g, 0.5 mmol), 1,4-dicyanobenzene (0.07 g, 0.5 mmol), 1,10-phenanthroline

DOI: 10.1039/b102888j

**Table 1** Structure determination summary for **1**–**5**

| Compound | **1** | **2** | **3** | **4** | **5** |
|---|---|---|---|---|---|
| Empirical formula | $C_{20}H_{14}CoN_2O_5$ | $C_{20}H_{12}CuN_2O_4$ | $C_{20}H_{14}ZnN_2O_5$ | $C_{20}H_{12}MnN_2O_4$ | $C_{16}H_{10}CdClN_2O_2$ |
| Formula weight | 421.27 | 407.86 | 427.70 | 399.26 | 410.13 |
| Space group | $P\bar{1}$ | $Cc$ | $P\bar{1}$ | $Cc$ | $C2/c$ |
| $a$/Å | 9.279(1) | 15.286(7) | 9.1894(4) | 17.510(6) | 23.099(3) |
| $b$/Å | 10.3777(9) | 10.143(3) | 10.5765(5) | 10.394(3) | 10.5089(5) |
| $c$/Å | 11.271(3) | 10.490(4) | 11.5636(6) | 9.373(4) | 16.804(2) |
| $\alpha$/° | 112.207(2) | 90 | 114.6210(10) | 90 | 90 |
| $\beta$/° | 94.849(3) | 93.77(3) | 91.562(2) | 95.88(2) | 133.783(3) |
| $\gamma$/° | 114.170(4) | 90 | 115.1470(10) | 90 | 90 |
| $V$/Å$^3$ | 879.2(2) | 1622.9(11) | 895.91(7) | 1696.9(10) | 2844.6(4) |
| $Z$ | 2 | 4 | 2 | 4 | 8 |
| $D_c$/g cm$^{-3}$ | 1.591 | 1.669 | 1.585 | 1.563 | 1.915 |
| $T$/K | 193(2) | 293(2) | 293(2) | 293(2) | 193(2) |
| $\mu$/mm$^{-1}$ | 1.013 | 1.377 | 1.406 | 0.808 | 1.732 |
| $\lambda$/Å (Mo-K$\alpha$) | 0.71069 | 0.71073 | 0.71073 | 0.71073 | 0.71069 |
| $F$(000) | 430 | 828 | 436 | 812 | 1608 |
| 2$\theta$ range/° | 4–55 | 2.41–25.03 | 2.00–25.03 | 2.28–25.05 | 4–55 |
| Independent reflections | 3961 | 1999 | 3135 | 1706 | 3416 |
| Observed reflections | 3450 | 1998 | 3134 | 1705 | 3178 |
| Variables | 253 | 244 | 309 | 244 | 199 |
| $R(F_o)$ | 0.031 | 0.0405 | 0.0444 | 0.0454 | 0.015 |
| $R_w(F_o)$ | 0.041 | 0.0798 | 0.0557 | 0.1056 | 0.025 |
| $S$ | 2.52 | 1.063 | 1.053 | 1.054 | 1.89 |
| Largest difference peak and hole/e Å$^{-3}$ | 0.39, −0.21 | 0.312, −0.261 | 0.840, −0.680 | 0.442, −0.424 | 0.33, −0.29 |

(0.1 g, 0.5 mmol) and $H_2O$ (16 ml) in the molar ratio of *ca.* 1 : 1 : 1 : 1777 was sealed in a 25 ml stainless-steel reactor with Teflon liner and was heated at 170 °C for 72 h. After cooling, prism-shaped yellow crystals of **4** were collected by filtration. Yield: 57%. Anal. Calc. for $C_{20}H_{12}MnN_2O_4$: C, 60.17; H, 3.03; N, 7.02%. Found: C, 60.76; H, 3.14; N, 7.28%. IR (KBr, cm$^{-1}$): 3385(br, vs), 1599(vs), 1387(vs), 847(m), 806(m), 750(s), 729(m), 505(m).

**[Cd(ta)$_{1/2}$(phen)Cl]$_n$ 5.** A mixture of $CdCl_2{\cdot}5H_2O$ (0.12 g, 0.5 mmol), 1,4-dicyanobenzene (0.07 g, 0.5 mmol), 1,10-phananthroline (0.1 g, 0.5 mmol) and $H_2O$ (16 ml) in the molar ratio of *ca.* 1 : 1 : 1 : 1777 was sealed in a 25 ml stainless-steel reactor with Teflon liner and was heated at 170 °C for 72 h. After cooling, block, colorless crystals of **5** were collected by filtration. Yield: 60%. Anal. Calc. for $C_{16}H_{10}CdN_2O_2Cl$: C, 46.86; H, 2.46; N, 6.83%. Found: C, 46.94; H, 2.46; N, 6.86%. IR (KBr, cm$^{-1}$): 3385(br, vs), 1570(vs), 1398(vs), 1144(m), 858(s), 744(s), 729(s), 507(m).

### Crystallography

Single crystals of complexes **1**–**5** with approximate dimensions 0.25 × 0.25 × 0.15 (**1**), 0.50 × 0.20 × 0.16 (**2**), 0.40 × 0.20 × 0.10 (**3**), 0.40 × 0.20 × 0.20 (**4**), 0.20 × 0.20 × 0.15 (**5**) mm were used for data collections. For **2**–**4**, data collections were performed on a Siemens Smart CCD diffractometer with graphite-monochromated Mo-K$\alpha$ radiation ($\lambda = 0.71073$ Å) at room temperature. Empirical absorption corrections were applied using the SADABS program[13] for the Siemens area detector. For **1** and **5**, because the thermal parameters of some atoms are not very well behaved, different data sets were collected on Siemens Smart CCD diffractometer at room temperature and Rigaku Rasa-7 CCD diffractometer at −80 °C. The latter data sets were used in this paper and empirical absorption correction was made with the 4th3D + 4th2D method for the Rigaku area detector. The structures of **2**–**4** were solved by direct methods and all calculations were performed by using the SHELXL PC program on a Legend computer.[14a] For **2** and **3**, the coordinates of the heavy atoms were obtained from an E-map; successive difference Fourier syntheses gave all the coordinates of other atoms, including H atoms. The structures were refined by full-matrix, least squares minimizations of $\Sigma(F_o - F_c)^2$ with anisotropic thermal parameters for all atoms except the H atoms. For **4**, the coordinates of the heavy atoms were obtained from an E-map; successive difference Fourier syntheses gave all the coordinates of the non-hydrogen atoms. The positions of H atoms were generated geometrically, assigned isotropic thermal parameters, and allowed to ride on their parent carbon atoms before the final cycle of refinement. The structure was refined by full-matrix, least squares minimization of $\Sigma(F_o - F_c)^2$ with anisotropic thermal parameters for all atoms except the H atoms. For **1** and **5**, the structures were solved by direct methods and all calculations were performed on a Silicon Graphics computer station with the teXsan program package.[14b] The positions of H atoms were generated geometrically and allowed to ride on their parent carbon atoms. The structure was refined by full-matrix, least squares with anisotropic thermal parameters for all atoms except the H atoms. Table 1 summarizes the important crystal data and Table 2 gives the selected bond lengths and angles for **1**–**5**.

CCDC reference numbers 151561–151565.

See http://www.rsc.org/suppdata/dt/b1/b102888j/ for crystallographic data in CIF or other electronic format.

### Physical measurements

The infrared spectra were taken on a Magna 750 FTIR spectrophotometer as KBr pellets in the 4000–400 cm$^{-1}$ region. The elemental analyses were performed in this institute. Variable-temperature magnetic susceptibility data for polycrystalline samples of complexes **1**, **2** and **4** were obtained in an external field of 10.0 kG on a Quantum Design PPMS Model 6000 magnetometer from 275 to 4 K.

## Results and discussion

### Preparation of the complexes

The reactions of 1,4-dicyanobenzene, 1,10-phananthroline and Co(II), Cu(II), Zn(II), Mn(II), Cd(II) salts by a hydrothermal method resulted in complexes **1**–**5** in yields from 57 to 70%. According to their crystal structures, they are ta-bridged polymeric complexes. It is clear that 1,4-dicyanobenzene is hydrolyzed to terephthalic acid during the reactions, similar to the work reported by Fun *et al.*[6]

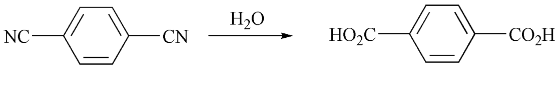

Cano *et al.* have reported reactions using ta as an initial regent in methanol: they isolated dimmeric Co(II), Cu(II)

**Table 2** Selected bond lengths (Å) and angles (°) for **1**–**5**

| | | | |
|---|---|---|---|
| **1**[a] | | | |
| Co–O(1) | 2.005(1) | Co–N(2) | 2.094(2) |
| Co–O(3) | 2.040(1) | Co–N(1) | 2.143(2) |
| Co–O(5) | 2.061(1) | | |
| O(3)–Co–O(1) | 99.42(6) | O(5)–Co–N(2) | 125.42(6) |
| O(3)–Co–O(5) | 89.05(6) | O(3)–Co–N(1) | 168.01(6) |
| O(1)–Co–O(5) | 139.32(6) | O(1)–Co–N(1) | 89.64(6) |
| O(3)–Co–N(2) | 92.95(6) | O(5)–Co–N(1) | 89.30(6) |
| O(1)–Co–N(2) | 94.03(6) | N(2)–Co–N(1) | 78.15(6) |
| **2**[b] | | | |
| Cu–O(4a) | 1.912(9) | Cu–N(1) | 2.003(11) |
| Cu–O(2) | 1.948(9) | Cu–N(2) | 2.032(10) |
| O(4a)–Cu–O(2) | 95.23(11) | O(4a)–Cu–N(2) | 173.2(4) |
| O(4a)–Cu–N(1) | 92.2(4) | O(2)–Cu–N(2) | 91.4(4) |
| O(2)–Cu–N(1) | 172.5(4) | N(1)–Cu–N(2) | 81.10(13) |
| **3**[a] | | | |
| Zn–O(1) | 2.003(2) | Zn–N(1) | 2.109(3) |
| Zn–O(3) | 2.023(2) | Zn–N(2) | 2.178(3) |
| Zn–O(5) | 2.053(3) | | |
| O(1)–Zn–O(3) | 97.44(11) | O(5)–Zn–N(1) | 127.27(12) |
| O(1)–Zn–O(5) | 130.95(11) | O(1)–Zn–N(2) | 94.70(11) |
| O(3)–Zn–O(5) | 87.42(12) | O(3)–Zn–N(2) | 165.14(11) |
| O(1)–Zn–N(1) | 101.47(11) | O(5)–Zn–N(2) | 91.09(13) |
| O(3)–Zn–N(1) | 91.60(11) | N(1)–Zn–N(2) | 77.57(11) |
| **4**[c] | | | |
| Mn–O(4c) | 2.105(10) | Mn–O(2a) | 2.150(8) |
| Mn–O(1) | 2.145(9) | Mn–N(1) | 2.336(11) |
| Mn–O(3b) | 2.144(7) | Mn–N(2) | 2.395(9) |
| O(4c)–Mn–O(1) | 97.8(3) | O(3b)–Mn–N(1) | 86.0(4) |
| O(4c)–Mn–O(3b) | 85.8(4) | O(2a)–Mn–N(1) | 164.9(4) |
| O(1)–Mn–O(3b) | 174.69(10) | O(4c)–Mn–N(2) | 165.6(4) |
| O(4c)–Mn–O(2a) | 99.55(13) | O(1)–Mn–N(2) | 85.9(3) |
| O(1)–Mn–O(2a) | 84.6(3) | O(3b)–Mn–N(2) | 89.7(4) |
| O(3b)–Mn–O(2a) | 98.6(3) | O(2a)–Mn–N(2) | 94.6(3) |
| O(4c)–Mn–N(1) | 95.1(4) | N(1)–Mn–N(2) | 70.95(12) |
| O(1)–Mn–N(1) | 89.8(4) | | |
| **5**[d] | | | |
| Cd–O(1b) | 2.207(1) | Cd–N(1) | 2.409(1) |
| Cd–O(2) | 2.309(1) | Cd–Cl(a) | 2.6132(4) |
| Cd–N(2) | 2.345(1) | Cd–Cl | 2.6671(5) |
| O(1b)–Cd–O(2) | 94.81(5) | O(1b)–Cd–N(1) | 103.89(5) |
| O(1b)–Cd–N(2) | 171.84(5) | O(2)–Cd–N(1) | 105.47(5) |
| O(5)–Cd–N(2) | 81.97(5) | N(2)–Cd–N(1) | 70.01(5) |
| O(1b)–Cd–Cl(a) | 95.83(4) | O(2)–Cd–Cl | 171.14(3) |
| O(2)–Cd–Cl(a) | 88.58(3) | N(2)–Cd–Cl | 94.54(4) |
| N(2)–Cd–Cl(a) | 91.60(4) | N(1)–Cd–Cl | 80.75(3) |
| N(1)–Cd–Cl(a) | 154.49(4) | Cl(a)–Cd–Cl | 83.37(1) |
| O(1b)–Cd–Cl | 89.68(4) | | |

[a] Symmetry transformations used to generate equivalent atoms: #1 $-x + 1, -y + 3, -z + 1$; #2 $-x - 1, -y + 2, -z$. [b] #1 $x - 1/2, -y - 1/2, z - 1/2$; #2 $x + 1/2, -y - 1/2, z + 1/2$. [c] #1 $x - 1/2, -y - 1/2, z - 1/2$; #2 $x -1/2, y + 1/2, z$; #3 $x, -y, z - 1/2$; #4 $x, -y, z + 1/2$; #5 $x + 1/2, -y - 1/2, z + 1/2$; #6 $x + 1/2, y - 1/2, z$. [d] #1 $-x, y, -z + 1/2$; #2 $-x, -y + 2, -z + 1$; #3 $-x - 1/2, -y + 5/2, -z$.

and Mn(II) complexes accompanied by insoluble polymers.[7] Recently, Chen and coworkers isolated three polymeric complexes from the hydrothermal reactions of 4,4′-bipy, $Na_2ta$ and metal nitrates.[15] In our system, if $Na_2ta$ was used as a reactant, the reactions resulted in insoluble precipitates or microcrystals. It is reasonable that the unsatisfactory results were induced by the high coordination ability of the carboxylate in $ta^{2-}$, leading the difficulty of crystal growth. When 1,4-dicyanobenzene was used, terephthalic acid and the complexes might be formed simultaneously, and the polymeric complexes in crystalline form were successfully isolated in high yield under hydrothermal conditions.

In an attempt on the preparation of polymers with different structures, the reactions of $MCl_2$ [or $M(OAc)_2$], 1,4-dicyanobenzene and phen with different molar ratios were carried out; however, the same results were obtained although the yields were different, illustrating that the compounds isolated in this reaction system are the most stable form under hydrothermal conditions. It is interesting, when $Cu(ClO_4)_2$ was used as a reactant, that a dinuclear copper compound $[Cu_2(phen)_4(ta)][ClO_4]_2$, which has a similar structure to $[Cu_2(bipy)_4(ta)][ClO_4]_2$,[7] was obtained in high yield.[12] Although detailed study is still needed, the difference in the structures may be caused by different anions in the reactions. When $Cu(ClO_4)_2$ is used, $Cu^{2+}$ is easily coordinated by two phen ligands and then bridged by ta, leading the formation of the dinuclear complex owing to the presence of non-coordinating anion $[ClO_4]^-$. When metal halide or acetate is used as reactant, the presence of coordinating anions $Cl^-$ or $OAc^-$ may render the easy coordination of two phen ligands to a same metal atom, and the coordinated anions may be replaced by ta to yield the formation of polymeric structures; the presence of coordinated Cl in **5** may support this speculation.

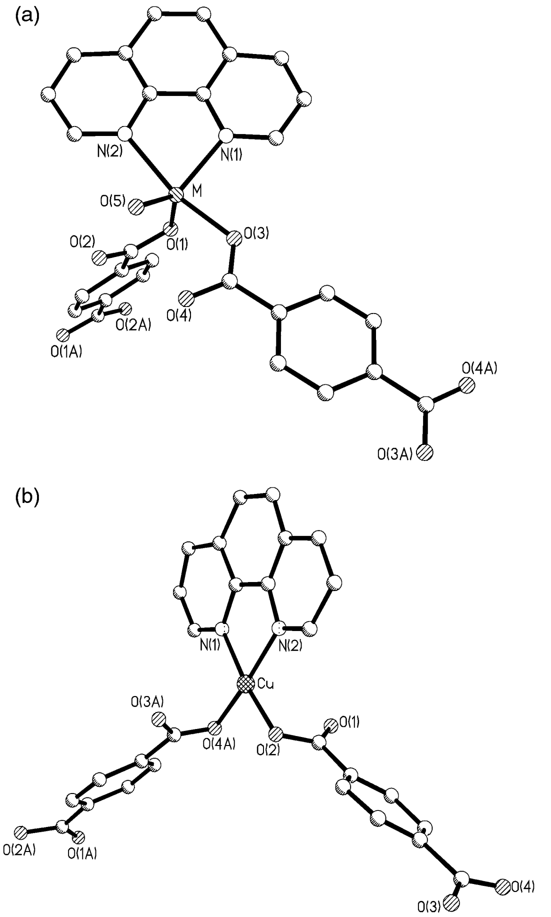

**Fig. 1** Local coordination environment around metal atoms (a) for **1** and **3**, (b) for **2**.

## Crystal structures

The structures of complexes **1**–**3** are very similar, being made up of one-dimensional zig-zag chain structures. Complexes **1** and **3** are isostructural, one coordinated water molecule per metal ion is present in the structure. The metal environment [Fig. 1(a)] can be best described as highly distorted trigonal bipyramidal with two nitrogen atoms from phen, two

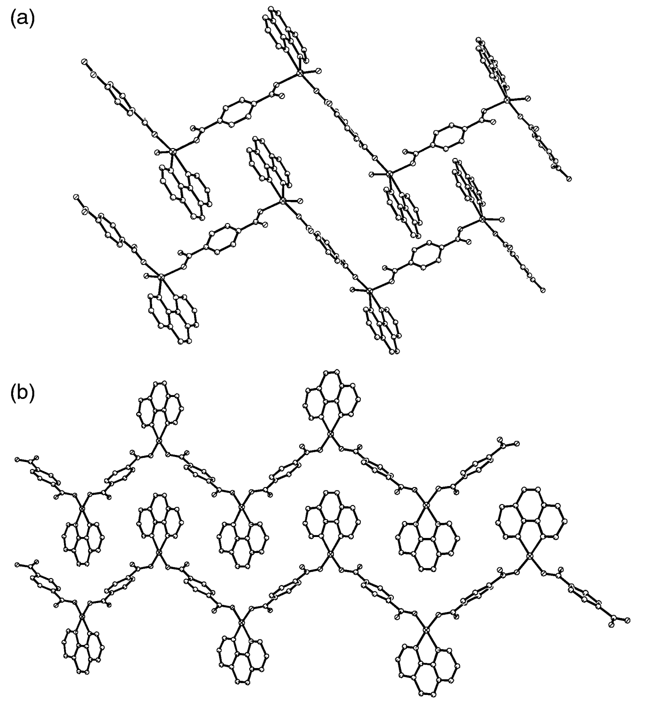

**Fig. 2** The 1-D chain structures along the *b* axis (a) for **1** and **3**, (b) for **2**.

carboxylato-oxygen atoms from different ta ligands and one oxygen atom from the coordinated water molecule. One nitrogen [N(1)] and one carboxylato-oxygen [O(3)] occupy the axial positions, whereas another nitrogen [N(2)] and two oxygens [O(5), O(1)] comprise the equatorial plane; the metal atom shows slight deviation from the plane (0.1246 Å for **1** and 0.0651 Å for **3**). The axial M–N and M–$O_{ta}$ distances are slightly longer than the equatorial distances, as shown by Co–N(1) [2.143(2) Å] and Co–O(3) [2.040(1) Å] with respect to Co–N(2) [2.094(2) Å] and Co–O(1) [2.005(1) Å] in **1**, Zn–N(1) [2.178(3) Å] and Zn–O(3) [2.023(3) Å] relative to Zn–N(2) [2.109(3) Å] and Zn–O(1) [2.003(2) Å] in **3**.

The copper atom in **2** exhibits a distorted square planar geometry [Fig. 1(b)] with two nitrogen atoms from phen and two carboxylato-oxygen atoms from different tas. The deviation of the metal atom from the mean N(1)N(2)O(2)O(4a) plane is 0.0162 Å. However, the Cu–O(1) [2.734(2) Å] and Cu–O(3a) [2.655(2) Å] distances show some weak interaction between the copper and uncoordinated oxygen of ta ligands, which may be viewed as a semi-chelating coordination mode.[16] Thus, the environment of the copper atom in **2** can also be described as a somewhat distorted octahedron: the two phen nitrogens [N(1) and N(2)] and two carboxylato-oxygens from two tas [O(2) and O(4a)] comprise the equatorial plane, while the axial positions are filled by the other two carboxylato-oxygens [O(1) and O(3a)]; the axial Cu–O distances [2.734(2) and 2.655(2) Å] are extremely elongated compared with the equatorial Cu–O distances [1.912(9) and 1.949(9) Å].

Each ta ligand in **1**–**3** adopts a $\mu_2$-bridging mode (Scheme 1c) with a typically average M–O distance, and each phen ligand acting as a terminal ligand with a typical M–N distance and N–M–N chelating angles. Thus, each ta ligand links two metal centers and each metal center connects two ta ligands to form the zig-zag chain structure (Fig. 2); the remaining coordination positions of the metal atom are saturated by the terminal phen ligand and the water molecule. Metal–metal distances are 11.040, 10.853 and 11.094 Å for **1**–**3**, respectively.

Complex **4** possesses a three-dimensional network structure: the dinuclear $[Mn_2(phen)_2(ta)_4]$ species with interatomic distance of 4.810(2) Å may be viewed as the basic subunit for the structure; the Mn(II) atom is coordinated by two nitrogen atoms from phen and four oxygen atoms from different ta ligands in a distorted octahedron geometry (Fig. 3). The phen ligand acts as a typical chelating ligand terminally coordinating to the Mn(II) atom with the Mn–N distances ranging from 2.336(11) to 2.395(9) Å and the N–Mn–N angle being 71.95(12)°; the Mn–N distances are longer than those found in $[Mn_2(phen)_4(ta)(H_2O)]^{2+}$.[7] Each ta ligand adopts a $\mu_4$-bridging mode (Scheme 1f), linking four Mn(II) atoms, and each Mn(II) attaches to four ta ligands. The other carboxylato end of the bridging ta ligand in one $Mn_2$ subunit connects to another subunit, *i.e.* every two $Mn_2$ subunits are linked together by sharing their bridging ta ligands to form a linear chain. The ta ligands outside the chains further inter-connect the chains both by long and short bridges: long bridges (through the phenyl ring) connect the chains to give rise to a two-dimensional layer containing a regular rhombus, in which the apexes are occupied by Mn(II) atoms and the edges are formed by ta ligands; the short bridges (carboxylato end) connect the layers to generate the final three-dimensional structure with rhombus channels (Fig. 4). The channel has a

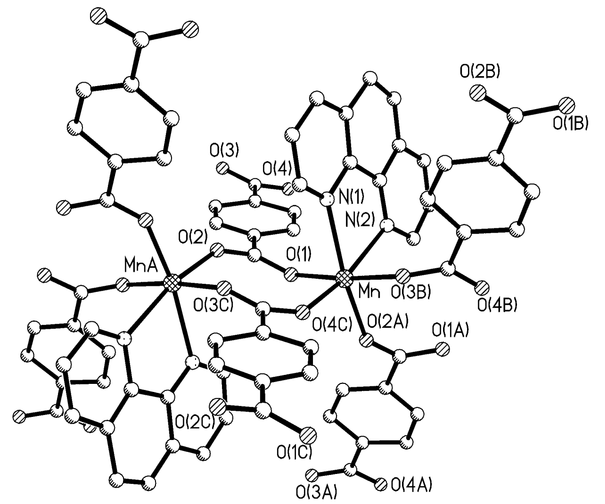

**Fig. 3** Local coordination environment around the Mn atom in **4**.

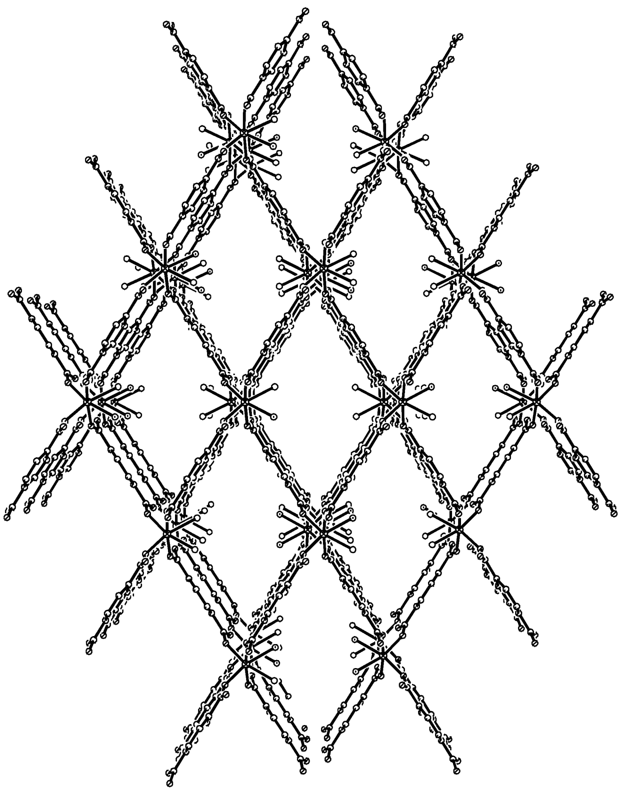

**Fig. 4** Packing structure along the *c* axis for **4**. Carbon atoms of phen are omitted for clarity.

diameter of 10.181 × 11.135 Å based on the Mn–Mn distance and is filled by phen ligands.

Complex **5** also has a three-dimensional structure: the coordination geometry of Cd(II) is a distorted octahedron completed by two nitrogen atoms from phen, two chloride atoms and two carboxylato-oxygen atoms (Fig. 5). Each phen acts as a typical chelating ligand terminally coordinating to the Cd(II) atom with the average Cd–N distance and N–Cd–N angle being 2.377(1) Å and 70.01(5)°, respectively. Similar to **4**, each ta ligands adopts a $\mu_4$-bridging mode (Scheme 1f), linking four Cd(II) centers. However, it is interesting that the Cd(II) atom only connects to two ta ligands, and the remaining coordination position is attached by a Cl atom that acts as a $\mu_2$-bridge linking two Cd atoms. Hence, the dinuclear $Cd_2(phen)Cl_2$ spices with an interatomic distance of 3.940(1) Å may be viewed as the subunit of the structure: two $Cd_2$ units are linked head-to-tail by a short bridge (carboxylato end) of one ta ligand, forming another subunit $[(Cd_2(phen)Cl_2)_2(ta)]$; two of the new subunits are connected face-to-face by two long-bridged ta ligands to form rectangular pores with a cavity of 10.51 × 11.85 Å. Each ta ligand is shared by four pores, generating a two-dimensional layer (Fig. 6a), different from the rectangular sheet in the Cd–ta–4,4′-bipy complex.[15a] The layers are further interconnected by long-bridged ta ligands, producing the three-dimensional structure. If viewed along the *c* axis, the structure can also be regarded as rectangular channels filled by phen ligands (Fig. 6b).

## Magnetic properties

Temperature-dependent magnetic susceptibility measurements for **1**, **2** and **4** were performed on polycrystalline samples. For complex **4**, the $\chi_M$ value increases as the temperature decreases, reaching a maximum of 0.1140 $cm^3 mol^{-1}$ at about 11 K, and then decreases on further cooling; the value of $\chi_M T$ is 4.2159 $cm^3 K mol^{-1}$ at room temperature and decreases continuously upon cooling; indicating the occurrence of antiferromagnetic interaction between the metal ions (Fig. 7). According to the structural data, the complex may exhibit two types of magnetic exchange interactions of Mn(II)–Mn(II): type one is through a short bridge *via* the carboxolato end of ta accompanying π–π interactions of phen along the *c* axis; and type two is through a long bridge *via* the phenyl ring of ta. Actually, the magnetic behavior is well interpreted based on the modified analytical expression [eqn. (1)],[17] which is derived from the Fisher model

$$\chi = \frac{Ng^2\mu_B^2}{3kT}\left(\frac{1+\mu_1+\mu_2+\mu_1\mu_2}{1-\mu_1\mu_2}\right) \quad (1)$$

where $\mu_1 = \coth(J_1/kT) - kT/J_1$, $\mu_2 = \coth(J_2/kT) - kT/J_2$.

By using a least squares method, a very satisfactory fit of the data at 5–300 K was obtained using the set of parameters of $J_1 = -2.02$ K, $J_2 = -1.69$ K and $g = 2.01$. The goodness of fit *R*, defined as

$$R = \frac{\Sigma[(\chi_M)_i^{obs} - (\chi_M)_i^{calc}]^2}{\Sigma(\chi_M)_i^{obs}} \quad (2)$$

is $1.0 \times 10^{-5}$. $J_1$ may be assigned to the antiferromagnetic exchange interaction of type one and $J_2$ to type two, the shorter Mn–Mn distance along with the π–π interactions of phen generate a stronger interaction $J_1$.

For complexes **1** and **2**, Fig. 8 shows the susceptibility curve of $\chi_M$ in the full temperature range, with the $1/\chi$ plot as an inset. The $\chi_M$ value decreases as temperature decreases; the values of $\chi_M$ are 0.0092 and 0.0013 $cm^3 mol^{-1}$ at room temperature for **1** and **2**, respectively. The $\chi_M$ data were fit to a modified Curie–Weiss law $\chi = \chi_0 + C/(T + \theta)$.[18] The calculated values of $C_m$ are 2.781, 0.337 and the Weiss temperatures, θ are −1.361 and −7.190 K for **1** and **2**, respectively.

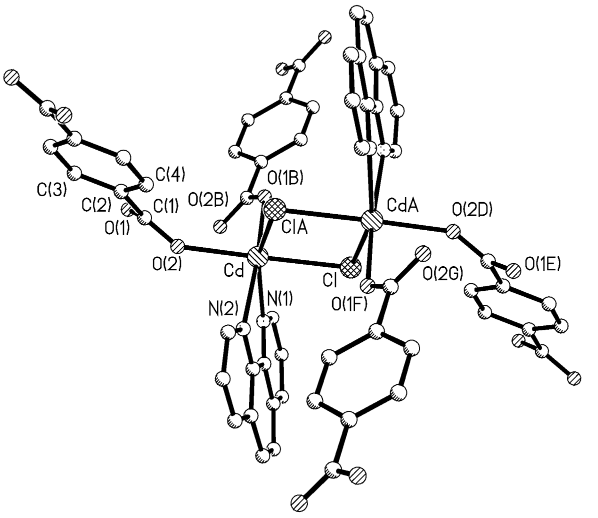

**Fig. 5** Local coordination environment around the Cd atom in **5**.

## Conclusion

We have systematically investigated the hydrothermal reactions of $MCl_2$ (M = Cu, Mn, Cd) or $M(OAc)_2$ (M = Co, Zn), 1,10-phenanthroline and 1,4-dicyanobenzene, and isolated five ta-bridged polymeric complexes in which the coordination geometries of the metal atoms are different except for the Co and Zn complexes. 1,4-Dicyanobenzene was hydrolyzed to terephthalic acid, resulting in good quality single crystals obtained in high yields for the five complexes. Also, the metal halides and acetates are helpful for the formation of polymeric

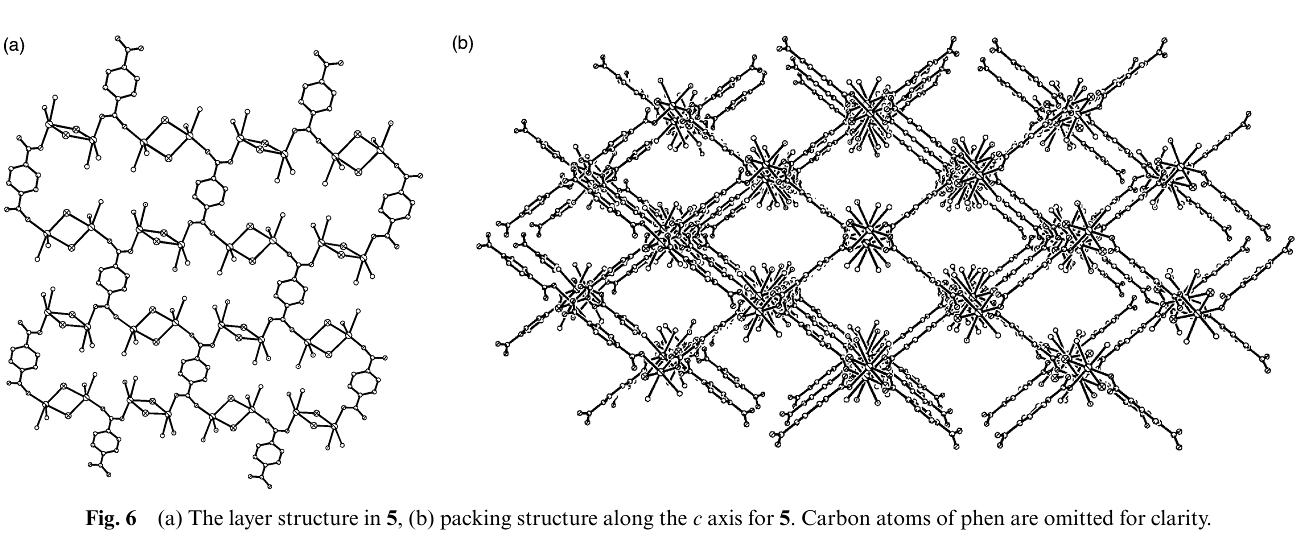

**Fig. 6** (a) The layer structure in **5**, (b) packing structure along the *c* axis for **5**. Carbon atoms of phen are omitted for clarity.

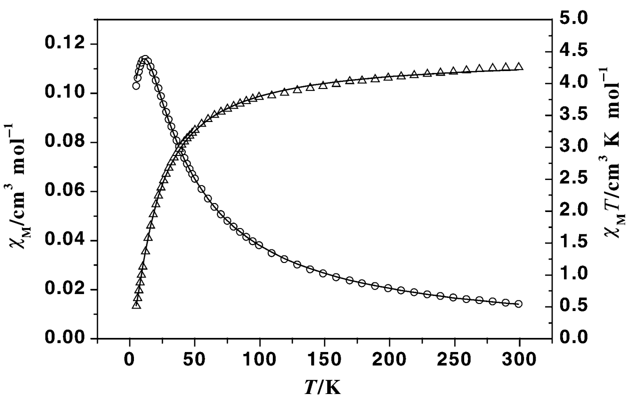

**Fig. 7** Experimental $\chi_M$ *versus* $T$ and $\chi_M T$ *versus* $T$ curves for complex **4**.

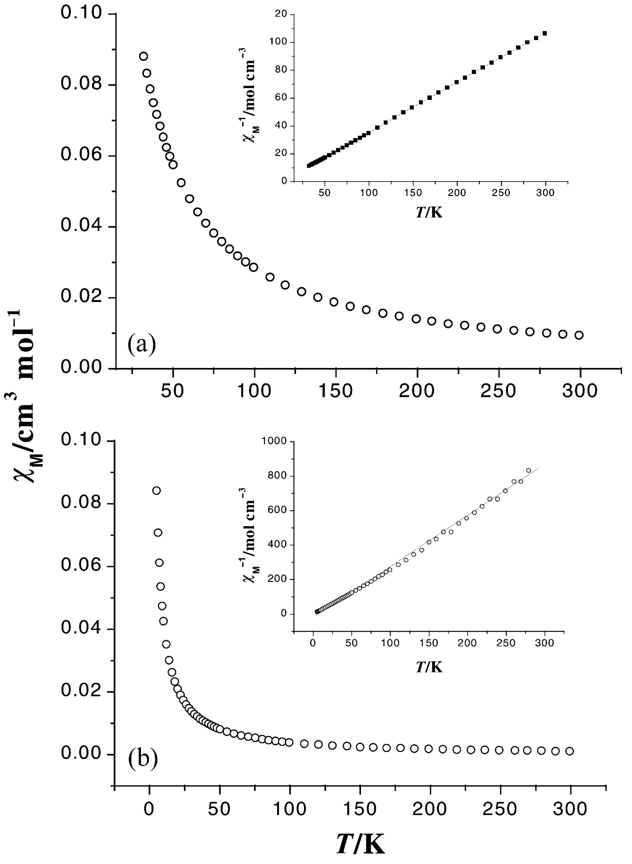

**Fig. 8** Experimental $\chi$ *versus* $T$ curves; insert is a plot of $1/\chi$ *versus* $T$ data (a) for **1**, (b) for **2**.

structures. The magnetic property studies suggest that metal–metal exchange interactions in Co, Cu and Mn complexes are antiferromagnetic, although in the cases of Co and Cu complexes this may be more complicated.

## Acknowledgements

The authors thank the financial support from NNSF of China and the Key Project from CAS.

## References

1 (*a*) H. O. Stumf, I. Oualmb, Y. Pei, D. Grandjean and O. Kahn, *Science*, 1993, **261**, 447; (*b*) H. Miyasaka, N. Matsumoto, H. Okawa, N. Re and E. Floriani, *Angew. Chem., Int. Ed. Engl.*, 1995, **34**, 1446; (*c*) J. Kim, M. Lim, Y. K. Choi and Y. Do, *Angew. Chem., Int. Ed. Engl.*, 1996, **35**, 993.

2 C. S. Hong, S. K. Son, Y. S. Lee, M. J. Jun and Y. Do, *Inorg. Chem.*, 1999, **38**, 5602.

3 (*a*) J. Cano, G. Demunno, J. L. Sanz, R. Ruiz, J. Faus, F. Lloret, M. Julve and A. Caneshi, *J. Chem. Soc., Dalton Trans.*, 1997, 1915; (*b*) E. G. Bakalbassis, J. Mrozaski and C. A. Tsipis, *Inorg. Chem.*, 1986, **25**, 3684; (*c*) M. Verdaguer, J. Gouteron, S. Jeannin, Y. Jeannin and O. Kahn, *Inorg. Chem.*, 1984, **23**, 4291.

4 (*a*) K. S. Bürger, P. Chaudhuri, K. Weighardt and B. Nuber, *Chem. Eur. J.*, 1995, **1**, 583; (*b*) P. Chaudhuri, K. Oder, K. Wieghardt, S. Gehring, W. Haase, B. Nuber and J. Weiss, *J. Am. Chem. Soc.*, 1988, **110**, 3657.

5 (*a*) C. E. Xanthopoulos, M. P. Sigala, G. A. Katsoulos, C. A. Tsipis, A. Terzis and M. Mentzafos, *Inorg. Chem.*, 1993, **32**, 5433; (*b*) E. G. Bakalbassis, A. P. Bozopoulos, J. Mrozinski, P. J. Rentzeperis and C. A. Tsipis, *Inorg. Chem.*, 1988, **27**, 529; (*c*) E. G. Bakalbassis, P. Bergerat, O. Kahn, S. Jeannin, Y. Jeannin, Y. Dromzee and M. Guillot, *Inorg. Chem.*, 1992, **31**, 625.

6 H. K. Fun, S. S. S. Raj, R. G. Xiong, J. L. Zuo, Z. Yu and X. Z. You, *J. Chem. Soc., Dalton Trans.*, 1999, 1915.

7 J. Cano, G. D. Munno, J. L. Sanz, R. Ruiz, J. Faus, F. Lloret, M. Julve and A. Caneschi, *J. Chem. Soc., Dalton Trans.*, 1997, 1915 and references therein.

8 R. M. Barrer, *The Hydrothermal Chemistry of Zeolites*, Academic Press, London, 1982.

9 P. J. Hagrman, D. Hagrman and J. Zubieta, *Angew. Chem., Int. Ed.*, 1999, **38**, 2638.

10 (*a*) A. Rabenau, *Angew. Chem., Int. Ed. Engl.*, 1985, **24**, 1026; R. A. Ludise, *Chem. Eng. News*, 1987, (Sept 28), 30; (*b*) J. Y. Lu, M. L. Lawandy, J. Li, T. Yuen and C. L. Lin, *Inorg. Chem.*, 1999, **38**, 2695 and references therein.

11 O. R. Evans, R. G. Xiong, Z. Wang, G. K. Wong and W. Lin, *Angew. Chem., Int. Ed. Engl.*, 1999, **38**, 536.

12 D. Sun, R. Cao, Y. Liang, M. Hong, W. Su and J. B. Weng, *Acta Crystallogr., Sect. C*, 2000, **56**, e240.

13 G. M. Sheldrick, SADABS, Program for Empirical Absorption Correction of Area Detector Data, University of Gottingen, Germany, 1996.

14 (*a*) G. M. Sheldrick SHELXL 93, Program for Crystal Structure Refinement, University of Gottingen, Germany, 1993; (*b*) teXsan: Crystal Structure Analysis Package, Molecular Structure Corporation, The Woodlands, TX, 1985 and 1992.

15 (*a*) J. Tao, M. L. Tong and X. M. Chen, *J. Chem. Soc., Dalton Trans.*, 2000, 3669; (*b*) S. M. F. Lo, S. S. Y. Chui, L. Y. Shek, Z. Lin, X. X. Zhang, G. Wen and I. D. Williams, *J. Am. Chem. Soc.*, 2000, **122**, 6293.

16 G. Guilera and J. W. Steed, *Chem. Commun.*, 1999, 1563.

17 R. Cortes, M. Drillon and S. Solans, *Inorg. Chem.*, 1997, **36**, 677.

18 X. X. Zhang, S. S.-Y. Chui and L. D. Williams, *J. Appl. Phys.*, 2000, **87**, 6007.